Research article

Chemotherapy induces an immunosuppressive gene expression signature in residual BRCA1/p53-deficient mouse mammary tumors

Sohvi Blatter[1], Nadine Stokar-Regenscheit[1], Ariena Kersbergen[2], Charlotte Guyader[2], Sven Rottenberg[1,3]*

[1] *Institute of Animal Pathology, Vetsuisse Faculty, University of Bern, Bern, Switzerland*
[2] *Division of Molecular Oncology, The Netherlands Cancer Institute, Amsterdam, The Netherlands*
[3] *Division of Molecular Pathology, The Netherlands Cancer Institute, Amsterdam, The Netherlands*

***Correspondence**: sven.rottenberg@vetsuisse.unibe.ch (Prof. Sven Rottenberg)

https://doi.org/10.31083/j.jmcm.2018.01.002

Abstract

Residual disease is a major hurdle in the eradication of human cancer. We have reproduced this by showing that mammary tumors arising in a mouse model for BRCA1-deficient breast cancer are also not easily eradicated by monotherapy with PARP inhibitors or platinum drugs, despite their high sensitivity to these cytotoxic agents. Tumor regrowth appears to originate from slowly cycling cells with a 2n DNA content that did not enter the $S/G_2/M$ phases of the cell cycle during treatment. To identify tumor-intrinsic mechanisms of drug resistance we characterized residual 2n tumor cells by RNAseq in our model. For this purpose, GFP-labelled 2n tumor cells were sorted from residual tumors after cisplatin treatment. We found that these cells display an increased expression of genes encoding immunosuppressive factors including IL-10 and TGF-β, as well as the negative costimulatory signals of the PD-1/PD-L1 and the CTLA-4/B7 axis. By blocking inhibitory T-cell signaling using antibodies directed against CTLA-4 and PD-1 in combination with cisplatin or PARP inhibitors, we attempted at overcoming the immunosuppressive microenvironment in BRCA1-deficient tumors and eradicate residual tumor cells. Expectedly, the combination of CTLA-4 and PD-1-targeting antibodies with the PARP-inhibitor olaparib led to an increase in CD8-positive cytotoxic T-cells in tumor remnants. Remarkably, this increase did not result in a therapeutic benefit and we were not able to eradicate the drug-tolerant tumor cells *in vivo* using this combination immunotherapy approach. This outcome might be due to other redundant immunosuppressive factors expressed by residual tumor cells as indicated by the increased number of tumor-infiltrating FoxP3-positive T-regulatory cells. Such adverse activation of T-regulatory cells upon immunotherapy may be relevant for the clinic and could explain some of the cases in which CTLA-4 and PD-1-blocking immunotherapy failed.

Keywords

BRCA1; Breast cancer; Residual disease; Immunotherapy; Immunosuppressive tumor signature; Immune checkpoint inhibition; Chemotherapy; PARP inhibition

Submitted: October 26, 2017; **Accepted:** November 6, 2017

1. Introduction

Homologous recombination (HR) deficiency constitutes an Achilles heel in *BRCA1*-mutated cancer, which can be exploited using platinum drugs [1] or PARP inhibitors [2–4]. In recent years it has been well established that breast and ovarian cancer patients carrying *BRCA1* mutations benefit from these DNA damage-inducing treatments [5–7]. Moreover, a substantial fraction of mutations causing HR defects are also seen in other tumor types, with advanced castration-resistant prostate cancer as a recent example [8]. In some patients with BRCA1-associated cancer, high-dose chemotherapy using alkylating agents appears to be curative [9, 10]. High-dose chemotherapy in breast cancer is only suitable for some patients, however, and standard chemotherapy usually does not cure patients with high-risk breast cancer [9, 10]. Even in drug sensitive tumors, relapse eventually occurs from residual tumor cells. The precise mechanisms that protect residual tumor cells from being killed are largely unclear.

Drug resistance can be mediated by intrinsic features of cancer cells *e.g.* epigenetic alterations or preexisting mutations in a heterogeneous population of cancer cells [11, 12]. Furthermore, cancer cells may acquire drug resistance due to mutations of the drug target, alterations in the DNA damage response, activation of parallel compensatory pathways by passing the inhibitory drug effect, decreased drug uptake, increased drug efflux, or altered cellular drug metabolism. Moreover, alterations in tumor microenvironment, *e.g.* hypoxic areas in tumors, may influence drug distribution and attenuate the cytotoxic drug effect on cancer cells [13, 14]. Intriguingly, alterations causing drug resistance might at the same time create vulnerabilities to other cytotoxic agents [15]. The identification of cellular modifications which increase sensitivity to a certain drug can influence the choice of treatment regimen and this Achilles heel may be exploited by new drug combinations, the development of novel compounds, or new ways of drug delivery [14, 16–20]. In addition to intrinsic or acquired drug resistance, transient drug tolerance causes minimal residual disease and prevents tumor eradication [21], as

exemplified by Sharma *et al.* [22] showing that cancer cells with an altered chromatin state are reversibly drug-tolerant.

To investigate the clinical hurdle of how *BRCA1*-mutated cancer cells escape eradication, we have turned to the *K14cre; Brca1*$^{F/F}$; *p53*$^{F/F}$ (KB1P) mouse model for hereditary breast cancer in which mammary tumors are highly sensitive to platinum-based chemotherapy or PARP inhibition [1, 4]. As with patients, the *Brca1*$^{-/-}$; *p53*$^{-/-}$ tumors are also not eradicated by these drugs and residual cells cause tumor relapse [23, 24]. In the KB1P model we recently showed that residual tumors consist of slowly cycling cells [24]. In particular, single nucleated cells with a 2n DNA content are transiently drug-resistant and give rise to tumor relapse [24]. How these residual tumor cells evade killing by the immune system is unknown. Exploring optimization of high-dose chemotherapy proved not possible in our mice, as we found that the organ limiting the dose in mice was not the bone marrow, as in humans, but the gut. We therefore turned to immunotherapy, as the residual tumor islets in our mouse tumors are embedded in a microenvironment containing various immune cells.

By performing RNAseq of KB1P tumors after cisplatin treatment, we found that residual tumor cells upregulate the expression of various genes encoding immunosuppressive factors, including PD-L1. The induction of these immunosuppressive pathways could be a critical factor that contributes to the lack of tumor eradication in our model. In recent years, immune checkpoint blockade has emerged as a new therapeutic approach resulting in tumor eradication in some patients who were previously considered incurable, *e.g.* patients suffering from metastatic melanoma or lung cancer [25, 26]. In particular, monoclonal antibodies that block the immune checkpoint receptors cytotoxic T lymphocyte–associated antigen 4 (CTLA-4) and programmed death-1 (PD-1), or its ligand PD-L1, stimulate the endogenous anti-tumor immune response [27]. By combining anti-PD-1 and anti-CTLA-4 antibodies inhibitory T-cell signaling is repressed at the stage of T-cell proliferation (anti-CTLA-4) and T-cell effector function (anti-PD-1) [28]. Immunotherapy targeting CTLA-4 and PD-1/PD-L1 is now state-of-the art therapy for the treatment of melanoma and lung cancer patients [29, 30]. A typical feature of these cancers is the high rate of mutation, providing many potential neo-antigens that can be detected by immune cells. A high mutation rate is also seen in triple-negative breast cancer, the molecular subtype that comprises *BRCA1*-mutated breast cancers. This high genomic instability is also a hallmark of the KB1P model [31]. However, the success of CTLA-4 and PD-1/PD-L1-targeting antibodies is thus far rather modest in triple-negative breast cancer [32–34]. We show here that the anti-PD-1 and anti-CTLA-4 antibodies did not result in tumor eradication either in our KB1P model, when combined with cisplatin or olaparib. Our unexpected finding of an increase in FoxP3-positive T-regulatory cells (Tregs) in the anti-PD-1/anti-CTLA-4- and olaparib-treated residual disease indicates the upregulation of compensatory immunosuppressive pathways, for example IL-10, TGF-β and NF-κB, which may impede the successful use of immunotherapy in the treatment of BRCA1-deficient cancer.

2. Materials and methods

2.1. Animal experiments

All experimental procedures were approved by the Animal Ethics Committee of the Netherlands Cancer Institute, Amsterdam, The Netherlands and the study was carried out in strict accordance with the Dutch and European regulations on care and protection of laboratory animals. *Brca1*$^{-/-}$*;p53*$^{-/-}$ mouse mammary tumors were generated in KB1P mice, which were backcrossed to an FVB/N background and transplanted into syngeneic mice as described previously [1, 31, 34]. All surgery was performed under ketamine, xylazine and acepromazine anesthesia and rimadyl was administered for pre- and postoperative analgesia to minimize suffering. Tumor volumes were calculated using caliper measurements (v=length* width^2*0.5). Tumor bearing mice were treated as indicated in the different experiments. 50 mg/mL stocks of olaparib (Syncom, The Netherlands) were diluted in DMSO with 10% 2-hydroxyl-propyl-β-cyclodextrine/PBS (final volume for injection 10 μL/g of body weight). Olaparib (50 mg/kg intraperitoneally (i.p.)) was injected daily. Cisplatin solution ready for injection was obtained from Mayne Pharma. Cisplatin (6 mg/kg intravenously (i.v.)) was injected once. Monoclonal anti-mouse CTLA-4 antibody (clone 9D9, BE0164, BioXCell) and monoclonal anti-mouse PD-1 antibody (clone RMP1-4, BE0146, BioXCell) were diluted in PBS immediately before administration and 100 μg were injected i.p. twice a week. The mice were euthanized by carbon dioxide when tumors reached a volume of 1500 mm^3 or at time points described in the different experiments. Tumors were subsequently harvested and further processed for RNA sequencing or immunohistochemistry (IHC).

2.2. RNA sequencing

Untreated and cisplatin-treated (7 days after treatment) GFP-expressing *Brca1*$^{-/-}$*;p53*$^{-/-}$ tumor cells were sorted [24] for GFP positivity and for 2n or 4n DNA content and total RNA was isolated from tumor cells using TRIZOL according to manufacturer's instructions (Invitrogen). Illumina RNA TruSeq Sample RNA sample preparation protocol [35] was used to prepare the samples and perform the high-throughput sequencing (Illumina HiSeq 2000). Standard Illumina indexing (index 7 bp) was included for multiplexing and single 50 bp reads were applied for deep sequencing. The R Stats package [36] was used for unsupervised hierarchical clustering and drawing of the heat map. The DESeq2 [37] package was used for differential expression analysis and DAVID functional annotation bioinformatics microarray analysis was used for GO-term analysis.

2.3. Immunohistochemistry

Antigen retrieval was performed by boiling the 10% formalin-fixed and paraffin embedded tumor samples for 20-30 min in TRIS/EDTA buffer (pH 9.0) (CD3, CD4, CD8) or citrate buffer (pH 6.0) (FoxP3). Slides were incubated at 4 °C overnight with the primary antibodies: monoclonal CD3 antibody (Neomarkers RM-9107-S, dilution: 1:600), monoclonal CD8 antibody (eBioscience 14-0808-82, dilution: 1:2000), monoclonal CD4 antibody (eBioscience 14-9766-82, dilution: 1:2000), monoclonal FoxP3 antibody (eBioscience 14-5773, dilution: 1:400), For secondary antibody labeling the slides were incubated with labeled polymer HRP anti-rabbit Envision (DakoCytomation K4011) (CD3), or a goat anti-rat-biotin antibody (Santa Cruz SC-2041, dilution: 1:100) followed by streptavidin/HRP (DakoCytomation P0397, dilution: 1:200) (CD4, CD8, FoxP3) for 30 min at room temperature. For detection, we used a standard procedure with DAB (Sigma, D-5905) and hematoxylin counterstaining. Positive and negative (only secondary antibody) controls were included for each staining procedure. Tumor infiltrating lymphocytes (TILs) were counted on 10 fields of 400 μm x 400

μm and the average numbers of cells per field were calculated. TILs were divided in three distribution patterns in the tumor: intratumoral (direct contact to tumor cells), adjacent stromal (intranodular stromal compartment, no direct contact to tumor cells) and distant stromal (extranodular stromal compartment) [38].

3. Results

3.1. *Residual tumor cells increase the expression of genes encoding immunosuppressive factors upon chemotherapy.*

To characterize residual tumor cells we have introduced the GFP marker into the BRCA1-deficient mouse model [24]. When tumor fragments of GFP-expressing BRCA1-deficient mice are transplanted into syngeneic mice, the GFP labeling allows us to distinguish the tumor cells from stromal cells for further analysis [24]. As usually seen in the KB1P model, the GFP-expressing BRCA1-deficient tumors are also sensitive to cisplatin therapy. They are not eradicated by the treatment and eventually relapse (Fig. 1A).

We then compared the gene expression profile of residual tumors 7 days after cisplatin therapy with that of saline-treated control tumors using RNAseq analysis. To achieve a tumor-specific profile, the GFP-positive cells were sorted out from the tumor for the RNAseq analysis. Since we recently showed that the drug-tolerant residual cells are enriched in the population that has a 2n DNA content [24], we further isolated 2n and 4n cells from 6 control (saline) or 9 residual (cisplatin) GFP-positive tumors before RNA extraction (Fig. 1B). Analysis of the gene expression profile of the control tumors using the gene ontology (G0) term "mitosis" confirmed the successful sorting of G_0/G_1 (2n) cells versus $S/G_2/M$ (4n) cells (Fig. 1C): the samples of cells with a 4n DNA content cluster together and highly express mitosis-related genes (shown in green), whereas cells with 2n DNA do not express these genes (shown in red). We then carried out an unsupervised hierarchical clustering analysis of all 30 samples. Fig. 1D shows that the residual 2n samples, which are enriched for the drug-tolerant tumor cells, clearly stand out from the other samples. This strongly suggests that they have a specific gene expression profile which distinguishes them from the other cell populations.

To identify specific gene expression signatures in residual tumors we compared the gene expression of the 2n cisplatin samples with that of the 2n control samples. This analysis identified various gene clusters that clearly separate the two groups (Fig. 2A). Consistent with our previous finding that the drug-tolerant cells are quiescent [24], the GO-term enrichment analysis of the differentially expressed genes showed a downregulation of biological processes related to cell cycle, cell division, mitosis, DNA replication and DNA damage response in the 2n cisplatin-treated cells (Fig. 2B, fold enrichment in blue, ranked by increasing *p*-value). Intriguingly, the GO-terms related to biological processes such as immune response, inflammation and angiogenesis were clearly increased in residual 2n cells (Fig. 2B, fold enrichment in red, ranked by increasing *p*-value). A more detailed analysis of upregulated pathways upon cisplatin therapy showed various immune-modulating factors to be activated in residual tumor cells, which apparently form an immunosuppressive tumor phenotype (Fig. 2C). The residual tumor cells are activating negative costimulatory signals of T-cells by upregulation of PD-L1, PD-L2, B7-1 and B7-2 expression. The immunosuppressive factors IL-10 and TGF-β as well as galectin 3 and 9, but not galectin 1 are upregulated. These factors negatively influence T-cell function [39–41]. IL-10 additionally impairs dendritic cell maturation [42]. Only prostaglandin E_2 (PGE_2), which has been shown to inhibit cytotoxic T-cell function [43], is downregulated in cisplatin-treated residual tumors. The death ligand TRAIL and the chemokine RANTES, which are involved in tumor-induced apoptosis of T-cells [44, 45] are also upregulated in residual tumors, as well as NF-κB, which protects tumor cells from apoptotic signaling via TRAIL [46]. SOCS1, which was shown to restrict antitumor activities of dendritic cells (DC) [47], is also upregulated upon cisplatin therapy.

Taken collectively, these data strongly suggest that the drug-tolerant KB1P remnants are not only quiescent, they also induce an immunosuppressive state by negatively influencing T-cells, DCs and by protecting tumor cells against apoptosis.

3.2. *Infiltration of residual tumors by T-lymphocytes is enhanced by immune checkpoint inhibition*

Given the increased gene expression of immunosuppressive factors, we hypothesized that residual tumor cells may evade eradication by immune cells. Therefore, we aimed to enhance the anti-tumor immune response by combining cisplatin or olaparib with the immune checkpoint inhibitory anti-PD-1 and anti-CTLA-4 antibodies. The *Brca1*$^{-/-}$; *p53*$^{-/-}$ tumors were transplanted into syngeneic mice and tumor-bearing mice were treated as shown in Fig. 3A. To test whether the applied immune checkpoint inhibition is effective in the KB1P model, we analyzed CD3-positive TILs using IHC in untreated tumors or in immunotherapy-treated residual tumors (7 days after cisplatin or 21 days after start of olaparib treatment). T-lymphocytes in different areas of the tumor have been associated with differential outcome of disease in breast cancer [48, 49]. Therefore, intratumoral lymphocytes were distinguished from lymphocytes in the adjacent or distant tumor stroma (Supplementary Fig. 1). Intratumoral lymphocytes were defined as cells with direct contact to tumor cells, adjacent stromal lymphocytes are in the intranodular stromal compartment with no direct contact to tumor cells, and distant stromal lymphocytes are in the extranodular stromal compartment. We identified T-lymphocytes (CD3-positive) infiltrating the untreated tumors. Our analysis of tumors after anti-cancer therapy showed that the number of TILs was significantly increased in residual tumors after treatment with the PARP inhibitor olaparib for 21 days, but not 7 days after cisplatin treatment. Adding immunotherapy to PARP inhibition increased the number of TILs in the residual tumors even further (Fig. 3B). CD3-positive T-cells were also increased in adjacent stroma of olaparib-treated tumors compared to untreated control tumors, but did not significantly change when immunotherapy was added (Supplementary Fig. 2A). Nevertheless, we were not able to increase TILs in the cisplatin-treated residual tumors by adding immune checkpoint inhibitors (Fig. 3B). This could be explained by the bone marrow toxicity of cisplatin, neutralizing the immune cell-activating effect of the immunotherapy 7 days after cisplatin therapy. Yet, the increase of CD3-positive TILs in tumor remnants treated with PARP inhibitors in combination with immune checkpoint inhibition suggests that this drug combination is useful to counteract the immunosuppressive tumor microenvironment.

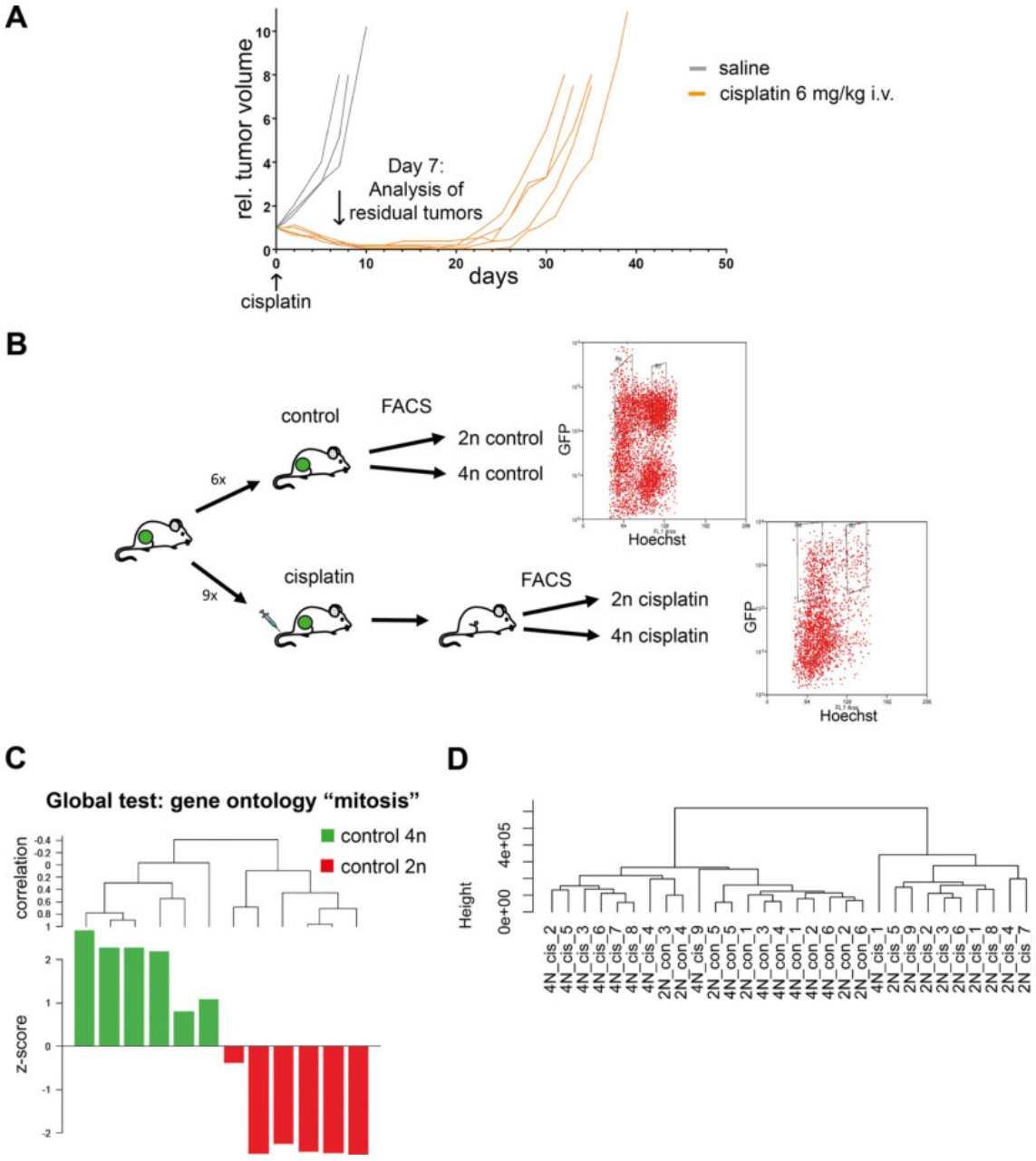

Fig. 1. RNAseq analysis of residual GFP expressing *Brca1*$^{-/-}$; *p53*$^{-/-}$ tumor cells. (A) Tumor growth and treatment response of BRCA1-deficient GFP-expressing tumors. Tumors were transplanted into 8 syngeneic mice and tumor-bearing mice were treated with 6 mg cisplatin per kg i.v. when tumors reached a volume of 200 mm^3 ($n = 5$) or left untreated ($n = 3$). (B) For RNAseq analysis, GFP-expressing *Brca1*$^{-/-}$; *p53*$^{-/-}$ tumors were transplanted into 15 mice. The mice were left untreated ($n = 6$) or treated with cisplatin (6 mg/kg i.v.) when tumors reached a volume of 200 mm^3 ($n = 9$). The untreated tumors were analyzed at a volume of about 1500 mm^3 and the cisplatin-treated residual tumors were analyzed 7 days after treatment. The GFP-positive BRCA1-deficient tumor cells were sorted for G_0/G_1 (2n DNA content) or $S/G_2/M$ (4n DNA content) and gene expression was quantified using RNAseq. (C) The global test algorithm [62] for the gene ontology term "mitosis" was performed on the sorted samples and separates the 2n from 4n samples. Green bars indicate a positive and red bars a negative Z score (D) Unsupervised hierarchical clustering of all samples of the RNAseq analysis. Gene expression in the residual cisplatin-treated tumor cells with 2n DNA content is distinct from gene expression in the other samples.

3.3. *Immune checkpoint inhibition in combination with cisplatin or PARP inhibitors does not eradicate residual BRCA1-deficient mammary tumors*

The increased TILs upon olaparib in combination with immunotherapy indicate that blocking PD-1 and CTLA-4 in combination with PARP inhibition is a promising approach to eradicate residual KB1P tumors. Although no increase in CD3-positive TILs was observed in Fig. 3, there may still be an immune-activating effect of immunotherapy in combination with cisplatin when the bone marrow has recovered beyond day 7. We therefore combined 100 μg PD-1 and CTLA-4 antibodies i.p. (twice a week, continuously) with 6 mg cisplatin per kg i.v. (day 0, Fig. 4A) or with 50 mg olaparib

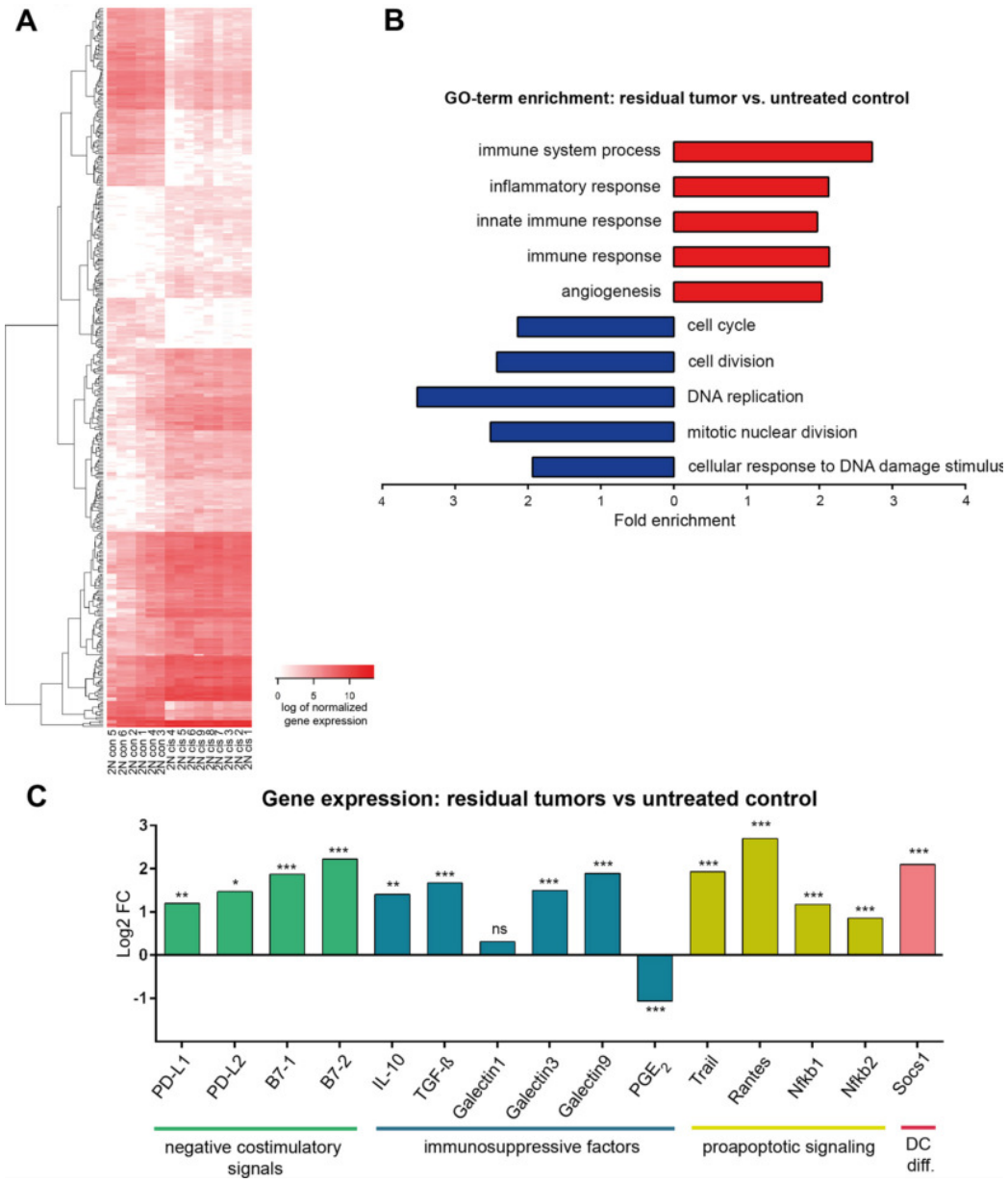

Fig. 2. Gene expression of immunosuppressive factors is upregulated in residual *Brca1*$^{-/-}$; *p53*$^{-/-}$ tumors. (A) Heat map showing differences in gene expression in tumor cells with 2n DNA content of untreated or cisplatin-treated KB1P GFP-expressing tumors. Genes with a 3-fold log2 change in gene expression and corrected $P < 0.001$ are shown. (B) GO-term enrichment analysis of upregulated and downregulated genes in residual *Brca1*$^{-/-}$; *p53*$^{-/-}$ tumor cells with 2n DNA content after cisplatin therapy compared to untreated tumor cells with 2n DNA content. The top 5 GO-terms enriched in upregulated and downregulated genes sorted by *p*-value are shown. The fold enrichment of upregulated biological processes is shown in red and the fold enrichment of downregulated biological processes is shown in blue. (C) Fold change (FC) in gene expression of selected immunoregulatory genes is shown comparing residual tumor cells with a 2n DNA content to untreated 2n tumor cells. Factors inducing an immunosuppressive microenvironment are upregulated in residual tumors (log2 FC > 0: higher expressed in residual tumors). Residual disease: $n = 9$; untreated control: $n = 6$. $*P < 0.05$, $**P < 0.01$, $***P < 0.001$, ns: non-significant.

per kg i.p. (daily for 28 days, Fig. 4C). As shown in Fig. 4B and 4D, we could not eradicate the BRCA1-deficient tumors or prolong relapse-free survival significantly by combining cisplatin or olaparib with PD-1 and CTLA-4 blocking antibodies. Furthermore, tumor growth was not inhibited by the addition of immunotherapy (Supplementary Fig. 3). Hence, the increase of TILs in tumor remnants upon immunotherapy in combination with olaparib or cisplatin was not sufficient to eradicate residual tumor cells in the KB1P model.

3.4. Immunotherapy enhances infiltration of CD8-positive cytotoxic T-cells but also FoxP3-positive regulatory T-cells in residual tumors after PARP inhibition.

To investigate the molecular mechanism underlying immun otherapy failure in this mouse model, we analyzed tumor-infiltrating CD8-posi- tive cytotoxic T-cells, CD4-positive T-helper cells and FoxP3-positive Tregs in residual tumors 7 days after cisplatin or

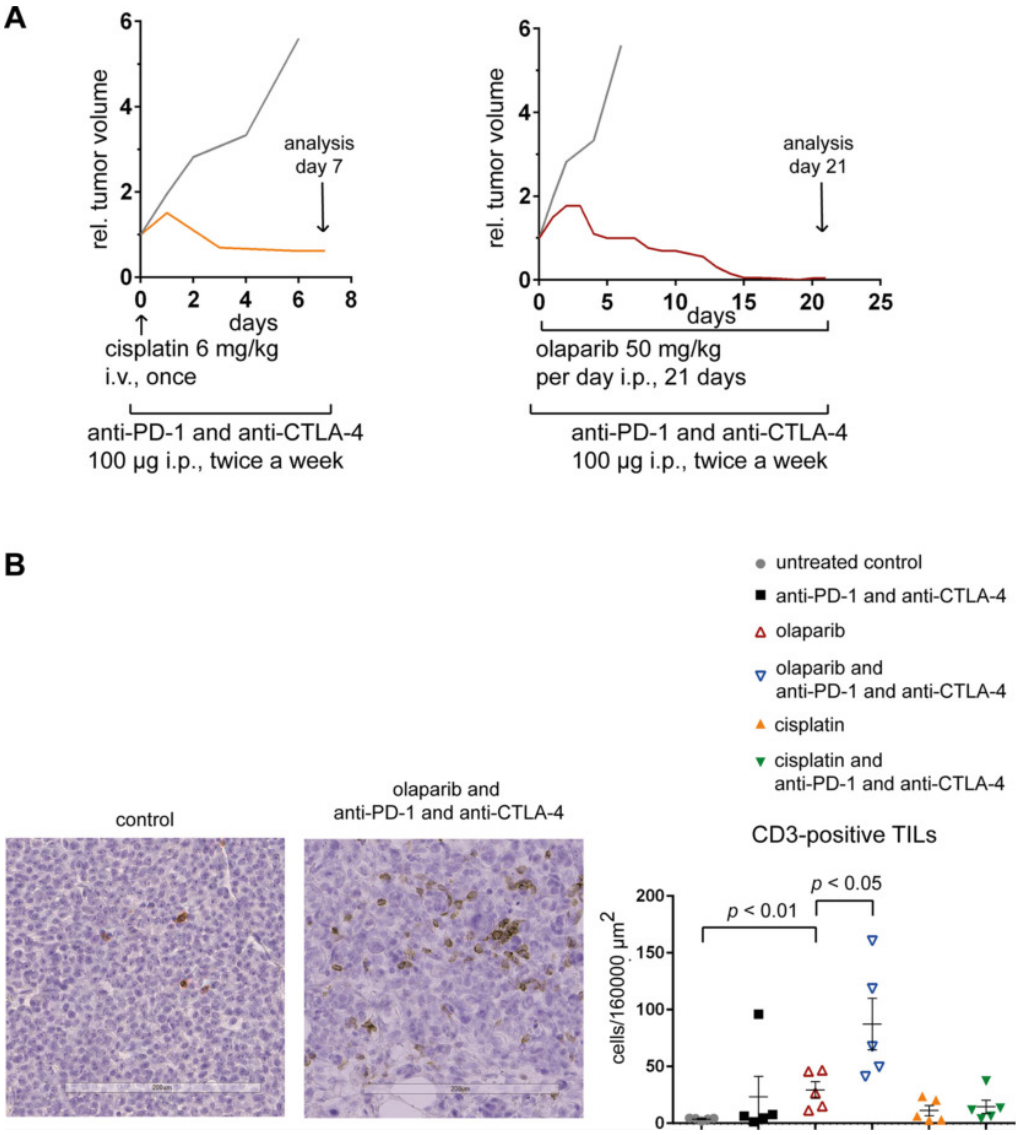

Fig. 3. Quantification of tumor-infiltrating T-cells in untreated and residual *Brca1*$^{-/-}$; *p53*$^{-/-}$ tumors. (A) Treatment scheme: *Brca1*$^{-/-}$;*p53*$^{-/-}$ tumors were transplanted into syngeneic mice and left untreated, treated with anti-PD-1 and anti-CTLA-4 antibodies (immunotherapy) starting at a tumor volume of about 60 mm^3, treated with cisplatin (6 mg/kg i.v.) at a tumor volume of 200 mm^3 (day 0), treated with olaparib (50 mg/kg per day i.p.) starting at a tumor volume of 200 mm^3, or combined treatment with cisplatin and immunotherapy or olaparib and immunotherapy. CD3-positive TILs were quantified in tumors when they reached a volume of about 1500 mm^3 (untreated control and immunotherapy alone) or residual tumors 7 days after cisplatin treatment or 21 days after treatment start with olaparib. (B) Quantification of CD3-positive intratumoral TILs using IHC. A representative IHC picture of an untreated control tumor and a tumor treated with olaparib in combination with anti-PD-1 and anti-CTLA-4 antibodies is shown. The average of TILs in 10 fields of 160000 μm^2 was quantified. $N = 5$ per treatment group. Error bars show SD. *P*-values were calculated using the two-tailed *t* test

21 days of olaparib treatment in combination with or without immunotherapy (Fig. 5A-C and Supplementary Fig. 2B-D). Again, we differentiated intratumoral, adjacent, and distant stromal TILs as described above.

In the distant stroma of residual tumors, we did not find any changes in TILs upon therapy (Supplementary Fig. 2). After cisplatin therapy, there was a slight increase of CD8 positive T-cells in adjacent stroma (Supplementary Fig. 2B). The TILs in the other tumor compartments did not change upon cisplatin therapy alone or in combination with immunotherapy (Fig. 5 and Supplementary Fig. 2). In contrast, various TILs increased upon olaparib treatment alone and even more upon combination treatment with the inhibitory anti-PD-1 and anti-CTLA-4 antibodies. The number of CD8-positive intratumoral as well as adjacent stromal TILs increased in olaparib-treated residual tumors and even a stronger increase was seen in tumor remnants when immunotherapy was added to PARP inhibition (Fig. 5A and Supplementary Fig. 2B). In contrast, CD4-positive T-cells did not increase upon olaparib monotherapy or its combination with immunotherapy (Fig. 5B and Supplementary Fig 2C). Interestingly, the number of intratumoral but not stromal FoxP3-positive Tregs increased markedly in residual tumors treated with olaparib in combination with immunotherapy compared to olaparib monotherapy (Fig. 5C and Supplementary Fig. 2D).

Taken altogether, this suggests that an increased number of

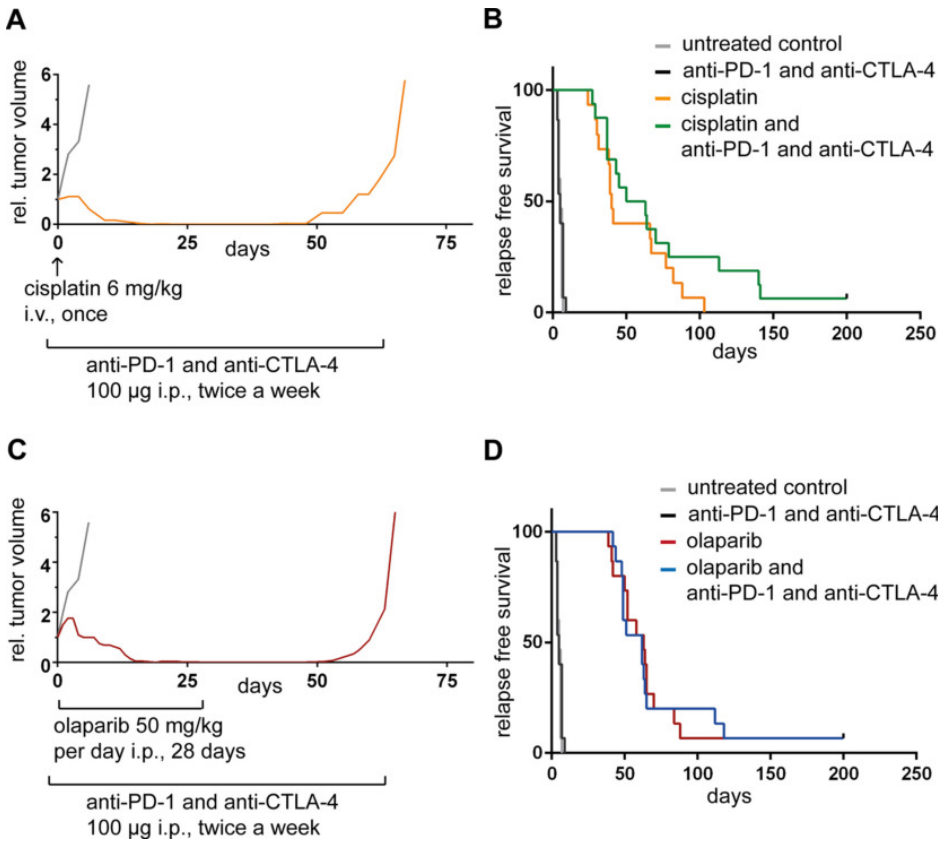

Fig. 4. Treatment response of *Brca1*$^{-/-}$; *p53*$^{-/-}$tumors to cisplatin or PARP inhibition in combination with immune checkpoint inhibition. Tumor pieces of 3 different donor tumors were transplanted into 5-6 mice per donor tumor and treatment group ($n = 15$ per treatment group). (A) Treatment scheme for immune checkpoint inhibition in combination with cisplatin: immunotherapy was started at tumor volumes of 60 mm^3. 100 μg of anti-PD-1 and anti-CTLA-4 antibodies were injected twice a week i.p. until the mice were sacrificed. Cisplatin treatment (6 mg/kg i.v. once) was started at a tumor volume of 200 mm^3. The mice were sacrificed when the relapsed tumor reached 4 times the volume at treatment start with cisplatin (time between day 0 until tumors reached 4 times the volume at treatment start: relapse free survival). (B) Relapse free survival of untreated, anti-PD-1 and anti-CTLA-4, cisplatin, and cisplatin and anti-PD-1 and anti-CTLA-4-treated mice is shown. There is no significant difference between treatment groups. (C) Treatment scheme for immune checkpoint inhibition in combination with PARP-inhibition: olaparib treatment was started at a tumor volume of 200 mm^3. 50 mg/kg olaparib was injected i.p. daily for 28 days. Immunotherapy was conducted as described in (A). Animals were sacrificed when tumors reached 4 times the volume at treatment start with olaparib (relapse free survival). (D) Relapse free survival of untreated, anti-PD-1 and anti-CTLA-4, olaparib or olaparib and anti-PD-1 and anti-CTLA-4-treated mice is shown. There is no significant difference between treatment groups.

FoxP3-positive Tregs may counteract the effect of immune checkpoint inhibition in residual disease and that this may contribute to the immunotherapy failure when combined with PARP inhibition.

4. Discussion

In this study, we found that residual tumor cells that are enriched for drug tolerance in the KB1P mouse model induce an immunosuppressive gene expression signature after DNA damage-inducing chemotherapy. Sorting of the GFP-expressing KB1P tumor cells followed by isolation of the 2n subpopulation of cells allowed us to characterize gene expression specifically in the residual tumor cell population enriched for cells that survive therapy and eventually repopulate the relapsing tumor. In particular, these cells displayed an upregulation of the expression of genes inhibiting T-cell function, inducing apoptosis of immune cells, inhibiting dendritic cell differentiation and genes activating negative costimulatory signals. An example of the latter is the negative costimulatory signaling of T-cells via the PD-L1/PD-1 and B7/CTLA-4 axis. It has been shown that PD-L1 expression is also upregulated upon PARP inhibition in breast cancer cell lines and xenograft tumors [50]. Therefore, PD-1 and CTLA-4 signaling may be an important target to overcome the immunosuppressive tumor microenvironment in breast cancer and prevent tumor relapse. Unexpectedly, the combination of olaparib or cisplatin with anti-CTLA-4 and anti-PD-1 antibodies did not eradicate residual *Brca1*$^{-/-}$; *p53*$^{-/-}$ mouse mammary tumors. This is consistent with the recent study by Nolan *et al*., in which no tumor eradication could be achieved in the *MMTVcre/Brca1*$^{fl/fl}$*p53*$^{+/-}$ model [51]. In contrast to the study of Nolan *et al* [51]. we did not observe an increase in the time until tumor relapse by combining PD-1 and CTLA-4 antibodies with cisplatin, which may be explained by the fact that we only used a single cisplatin dose.

Similar to these findings, the benefit of PD-1 and CTLA-4-targeting immunotherapy is also unexpectedly modest in human triple-nega- tive breast cancer [33], and the precise mechanisms underlying this poor outcome remain unclear. Using our KB1P model, we investigated whether the immune cell composition of the residual disease shortly after chemotherapy exposure may provide new hy-

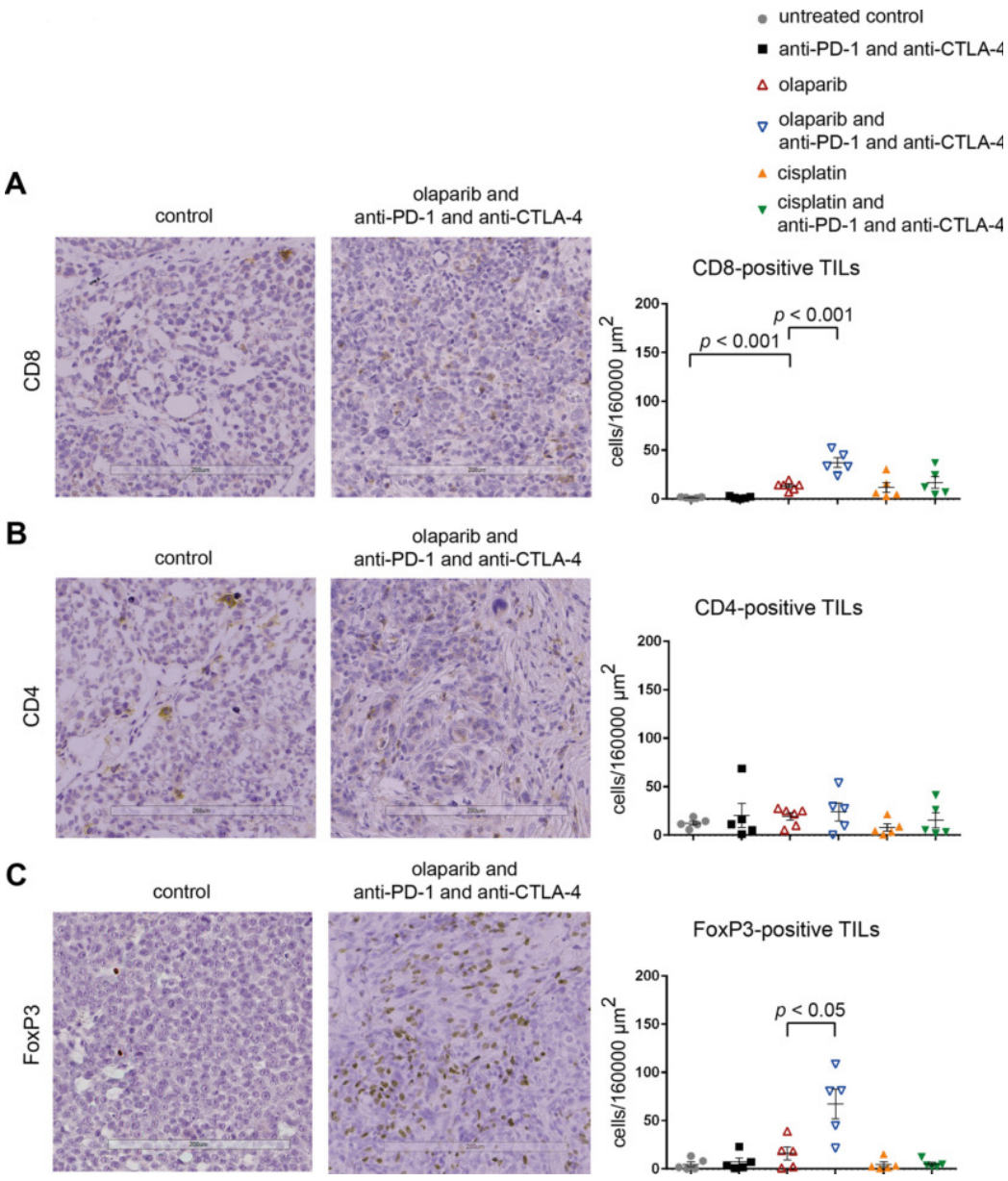

Fig. 5. Quantification of cytotoxic and regulatory TILs in residual *Brca1*$^{-/-}$; *p53*$^{-/-}$tumors. Intratumoral CD8-, CD4- and FoxP3-positive TILs were quantified as described in Fig. 3 in untreated control tumors (tumor volume: 1500 mm^3), anti-PD-1 and anti-CTLA-4-treated tumors (tumor volume: 1500 mm^3), olaparib-treated tumors (residual tumors 21 days after start of olaparib treatment), olaparib and anti-PD-1 and anti-CTLA-4-treated tumors (residual tumors 21 days after start of olaparib treatment), cisplatin-treated tumors (residual tumors 7 days after cisplatin treatment) and cisplatin and anti-PD-1 and anti-CTLA-4-treated tumors (residual tumors 7 days after cisplatin treatment). $N = 5$-6 per treatment group; error bars show SD. *P*-values were calculated using the two-tailed *t* test. For each staining a representative IHC picture of an untreated control tumor and a tumor treated with olaparib in combination with anti-PD-1 and anti-CTLA-4 antibodies is shown. (A) CD8-positive TILs (B) CD4-positive TILs (C) FoxP3-positive TILs

potheses to explain this conundrum. We found that the tumor infiltrating CD8-positive T-cell population was expanded upon olaparib treatment in combination with immunotherapy, but simultaneously FoxP3-positive Tregs accumulated in residual tumors despite CTLA-4-blockade. Combination of PD-1- and CTLA-4 blockade was shown to expand T-cells and to activate their effector function [28]. Moreover, Curran *et al.* [52] showed that tumor-infiltrating T-effector cells (Teffs) were expanded in melanomas in mice after combination treatment with anti-PD-1 and anti-CTLA-4 antibodies leading to an increased Teffs/Treg ratio and tumor rejection. Nevertheless, combining anti-CTLA-4 and anti-PD-1 antibodies is apparently not sufficiently increasing T-cell activity against residual BRCA1-deficient tumors in our model. Varying outcomes on T-cell activity have also been found by other groups. For example, anti-CTLA-4 antibodies were reported to directly deplete Tregs [53], whereas Khan *et al.* observed that CTLA-4-blockade activates Teffs rather than influencing Tregs [54]. Furthermore, Kavanagh *et al.* found that FoxP3-positive Tregs are even expanded when prostate cancer patients were treated with anti-CTLA-4 antibodies [55]. The accumulation of intratumoral Tregs that we also found in our model might have counteracted the

anti-tumor response of activated Teffs and the antagonistic effect of Tregs might similarly explain failure of immunotherapy in cancer patients.

In contrast to the combined treatment with chemotherapy and immunotherapy, the alkylating agent nimustine eradicates KB1P tumors [24]. Therefore, high-dose chemotherapy is another therapeutic option in addition to the combination of standard chemotherapy or PARP inhibition with immunotherapy for the treatment of patients with BRCA-deficient breast cancer [9, 10]. Nevertheless, to treat patients who are not eligible for high-dose chemotherapy, novel therapeutic strategies need to be explored to achieve tumor eradication. The efficacy of anti-cancer drugs in tumors may be enhanced by the use of novel technologies for delivery of drugs to the site of action, *e.g.* the use of nanovehicles [18]. Specifically designed nanovehicles may increase the uptake of drugs particularly in tumor cells and thereby allow the administration of higher doses of cytotoxic drugs without increasing the cytotoxic effect to normal cells. To deliver the drugs more specifically to cancer cells, there is an urgent need to identify proteins expressed on the cell membrane of drug-tolerant cells, which could serve as receptors for the uptake of nanoparticles.

To overcome the poor outcome of chemotherapy in combination with immunotherapy, targeting additional immunosuppressive pathways induced by cisplatin or by PARP inhibition may be a useful approach. Inhibiting NF-κB might increase cytotoxic T-cell activity in the residual BRCA1-deficient tumors and therefore mediate tumor regression [46]. Furthermore, inhibition of SOCS1 or modulation of antigen presenting cells (APCs), *e.g.* using tyrosine kinase inhibition [56] might break self-tolerance [47] and prevent failure of immunotherapy. Another promising but challenging approach is specifically target Tregs without compromising T-effector cell activity. CD25, the α-subunit of the IL-2 receptor, was considered a promising target for Treg cells, but it has not led to a successful treatment of established tumors, because activated Teffs that also express CD25 are simultaneously depleted [57]. IL-10 expands Tregs [58] and is upregulated in residual BRCA1-deficient tumors. Targeting IL-10 might therefore inhibit Treg cell expansion and might increase effectiveness of immune checkpoint inhibition. In our present mouse model, BRCA1-deficient residual tumor cells also upregulated TGF-β gene expression. The secretion of TGF-β was shown to induce Treg proliferation during tumor growth [59], and TGF-β inhibition resulted in the eradication of transplantable mouse tumors [60]. Furthermore, TGF-β inhibitors have been shown to restore an immune response in tumors and to increase the efficacy of combined immunotherapy [61]. Therefore, targeting TGF-β might be a promising approach to eradicate residual BRCA1-deficient tumor cells.

Further investigation into the immunosuppressive microenvironment induced by the residual mammary tumors in our BRCA1-deficient mouse model might reveal novel combination regimen with PARP inhibitors and immunomodulatory agents. The identification of such treatment regimens may then be useful to enhance checkpoint blockade therapy for patients with BRCA1-deficient breast cancer.

5. Supplementary material

Supplementary Dataset 1. Data of RNAseq experiment. Text file containing the raw sequencing counts of the RNAseq analysis of residual cisplatin-treated and untreated tumor cells with 2n or 4n DNA content. Treatment (cisplatin or untreated) and DNA content (2n or 4n) followed by sample number and donor tumor (tumor number 121 or 107) are indicated in the sample name.

Acknowledgments

We thank Karin de Visser and Seth Coffelt for scientific advice in experimental planning and Frank van Diepen for laboratory assistance. We thank the genomics core facility of the Netherlands Cancer Institute for the RNA sequencing and Iris de Rink for the help with processing the raw sequencing data. Moreover, we wish to thank Piet Borst and Nora Gerhards for critical reading of the manuscript. This work was supported by grants from the Netherlands Organization for Scientific Research (NWO-VIDI-91711302 to SR), the European Research Council (ERC-CoG-681572 to SR), the Swiss National Science Foundation (project grant 310030_156869 to SR) and the Swiss Cancer Research foundation (MD-PhD-3446-01-2014 to SB).

Conflict of Interest

There are no conflicts of interest stated by the authors.

Author Contributions

Experimental planning: Sven Rottenberg, Sohvi Blatter, Charlotte Guyader; Acquisition of data: Sohvi Blatter, Charlotte Guyade, Nadine Stokar-Regenscheit, Ariena Kersbergen, Sven Rottenberg; Analysis and interpretation of data: Sven Rottenberg, Sohvi Blatter, Nadine Stokar-Regenscheit; Writing and revision of the manuscript: Sven Rottenberg, Sohvi Blatter, Nadine Stokar-Regenscheit; Study supervision: Sven Rottenberg.

References

[1] Rottenberg S, Nygren AO, Pajic M, Van Leeuwen FW, Van DHI, Van DWK, *et al.* Selective induction of chemotherapy resistance of mammary tumors in a conditional mouse model for hereditary breast cancer. *P Natl Acad Sci USA*, 2007; 104(29): 12117-12122.

[2] Bryant HE, Schultz N, Thomas HD, Parker KM, Flower D, Lopez E, *et al.* Specific killing of BRCA2-deficient tumours with inhibitors of poly(ADP-ribose) polymerase. *Nature*, 2005; 434(7035): 913.

[3] Farmer H, McCabe N, Lord CJ, Tutt AN, Johnson DA, Richardson TB, *et al.* Targeting the DNA repair defect in BRCA mutant cells as a therapeutic strategy. *Nature*, 2005; 434(7035): 917-921.

[4] Rottenberg S, Jaspers JE, Kersbergen A, Van DBE, Nygren AO, Zander SA, *et al.* High sensitivity of BRCA1-deficient mammary tumors to the PARP inhibitor AZD2281 alone and in combination with platinum drugs. *P Natl Acad Sci USA*, 2008; 105(44): 17079-17084.

[5] Audeh MW, Carmichael J, Penson RT, Friedlander M, Powell B, Bell-Mcguinn KM, *et al.* Oral poly(ADP-ribose) polymerase inhibitor olaparib in patients with BRCA1 or BRCA2 mutations and recurrent ovarian cancer: a proof-of-concept trial. *Lancet*, 2010; 376(9737): 245-251.

[6] Silver DP, Richardson AA. Efficacy of neoadjuvant Cisplatin in triple-negative breast cancer. *J Clin Oncol*, 2010; 28(7): 1145-1153.

[7] Tutt A, Robson M, Garber JE, Domchek SM, Audeh MW, Weitzel JN, *et al.* Oral poly (ADP-ribose) polymerase inhibitor olaparib in patients with BRCA1 or BRCA2 mutations and advanced breast cancer: a proof-of-concept trial. *Lancet*, 2010; 376(9737): 235-244.

[8] Mateo J, Boysen G, Barbieri CE, Bryant HE, Castro E, Nelson PS, *et al.* DNA Repair in Prostate Cancer: Biology and Clinical Implications. *Eur Urol*, 2017; 71(3).

[9] Vollebergh MA, Lips EH, Nederlof PM, Wessels LFA, Schmidt MK, Beers EHV, *et al.* An aCGH classifier derived from BRCA1-mutated breast cancer and benefit of high-dose platinum-based chemotherapy in HER2-negative breast cancer patients. *Annu Oncol*, 2011; 22(7): 1561-1570.

[10] Vollebergh MA, Lips EH, Nederlof PM, Wessels LF, Wesseling J, Vijver MJV, *et al.* Genomic patterns resembling BRCA1- and BRCA2-mutated breast cancers predict benefit of intensified carboplatin-based chemotherapy. *Breast Cancer Res*, 2014; 16(3): R47.

[11] Zhang J, Fujimoto J, Zhang J, Wedge DC, Song X, Zhang J, *et al.* Intratumor heterogeneity in localized lung adenocarcinomas delineated by multiregion sequencing. *Science*, 2014; 346(6206): 256-259.

[12] Shaffer SM, Dunagin MC, Torborg SR, Torre EA, Emert B, Krepler C, *et al.* Rare cell variability and drug-induced reprogramming as a mode of cancer drug resistance. *Nature*, 2017; 546(7658): 431.

[13] Gottesman MM, Lavi O, Hall MD, Gillet JP. Toward a Better Understanding of the Complexity of Cancer Drug Resistance. *Annu Rev Pharmacol*, 2016; 56(1): 85.

[14] Wijdeven RH, Pang B, Assaraf YG, Neefjes J. Old drugs, novel ways out: Drug resistance toward cytotoxic chemotherapeutics. *Drug Resist Update*, 2016; 28: 65-81.

[15] Szakás G, Hall MD, Gottesman MM, Boumendjel A, Kachadourian R, Day BJ, *et al.* Targeting the Achilles Heel of Multidrug-Resistant Cancer by Exploiting the Fitness Cost of Resistance. *Chem Rev*, 2014; 114(11): 5753-5774.

[16] Li W, Zhang H, Assaraf YG, Zhao K, Xu X, Xie J, *et al.* Overcoming ABC transporter-mediated multidrug resistance: Molecular mechanisms and novel therapeutic drug strategies. *Drug Resist Update*, 2016; 27: 14-29.

[17] Zhitomirsky B, Assaraf YG. Lysosomes as mediators of drug resistance in cancer. *Drug Resist Update*, 2016; 24: 23-33.

[18] Livney YD, Assaraf YG. Rationally designed nanovehicles to overcome cancer chemoresistance. *Adv Drug Deliver Rev*, 2013; 65(13-14): 1716-1730.

[19] Shapira A, Livney YD, Broxterman HJ, Assaraf YG. Nanomedicine for targeted cancer therapy: towards the overcoming of drug resistance. *Drug Resist Update*, 2011; 14(3): 150-163.

[20] Gonen N, Assaraf YG. Antifolates in cancer therapy: Structure, activity and mechanisms of drug resistance. *Drug Resist Update*, 2012; 15(4): 183-210.

[21] Borst P. Cancer drug pan-resistance: pumps, cancer stem cells, quiescence, epithelial to mesenchymal transition, blocked cell death pathways, persisters or what? *Open Biol*, 2012; 2(5): 944-945.

[22] Sharma SV, Lee DY, Li B, Quinlan MP, Takahashi F, Maheswaran S, *et al.* A chromatin-mediated reversible drug-tolerant state in cancer cell subpopulations. *Cell*, 2010; 141(1): 69.

[23] Rottenberg S, Borst P. Drug resistance in the mouse cancer clinic. *Drug Resist Update*, 2012; 15(1-2): 81-89.

[24] Pajic M, Blatter S, Guyader C, Gonggrijp M, Kersbergen A, KüçüKosmanoğLu A, *et al.* Selected alkylating agents can overcome drug tolerance of G0-like tumor cells and eradicate BRCA1-deficient mammary tumors in mice. *Clin Cancer Res Off J Am Assoc Cancer Res*, 2017; 23(22): 7020-33.

[25] Hodi FS, O'day SJ, Mcdermott DF, Weber RW, Sosman JA, Haanen JB, *et al.* Improved Survival with Ipilimumab in Patients with Metastatic Melanoma. *New Engl J Med*, 2010; 363(8): 711-723.

[26] Reck M, Rodríguez-Abreu D, Robinson AG, Hui R, Csőszi T, Fülöp A, *et al.* Pembrolizumab versus Chemotherapy for PD-L1-Positive Non-Small-Cell Lung Cancer. *New Engl J Med*, 2016; 375(19): 1823.

[27] Topalian SL, Drake CG, Pardoll DM. Immune checkpoint blockade: a common denominator approach to cancer therapy. *Cancer Cell*, 2015; 27(4): 450.

[28] Mellman I, Coukos G, Dranoff G. Cancer immunotherapy comes of age. *Nature*, 2011; 480(7378): 480-489.

[29] Rotte A, Bhandaru M, Zhou Y, Mcelwee KJ. Immunotherapy of melanoma: Present options and future promises. *Cancer Metast Rev*, 2015; 34(1): 115.

[30] Anagnostou VK, Brahmer JR. Cancer immunotherapy: a future paradigm shift in the treatment of non-small cell lung cancer. *Clin Cancer Res*, 2015; 21(5): 976.

[31] Liu X, Holstege H, Van DGH, Treur-Mulder M, Zevenhoven J, Velds A, *et al.* Somatic loss of BRCA1 and p53 in mice induces mammary tumors with features of human BRCA1-mutated basal-like breast cancer. *P Natl Acad Sci USA*, 2007; 104(29): 12111-12116.

[32] Bianchini G, Balko JM, Mayer IA, Sanders ME, Gianni L. Triple-negative breast cancer: challenges and opportunities of a heterogeneous disease. *Nat Rev Clin Oncol*, 2016; 13(11): 674.

[33] Nanda R, Chow LQ, Dees EC, Berger R, Gupta S, Geva R, *et al.* Pembrolizumab in Patients With Advanced Triple-Negative Breast Cancer: Phase Ib KEYNOTE-012 Study. *J Clin Oncol*, 2016; 34(21): 2460.

[34] Jaspers JE, Kersbergen A, Boon U, Sol W, Deemter LV, Zander SA, *et al.* Loss of 53BP1 Causes PARP Inhibitor Resistance in Brca1-Mutated Mouse Mammary Tumors. *Cancer Discov*, 2013; 3(1): 68-81.

[35] Illumina inc. 2014. TruSeq ® RNA Sample Preparation v2 Guide. [ONLINE] Available at: *https://support.illumina.com/content/dam/illuminasupport/documents/documentation/chemistry_documentation/samplepreps_truseq/truseqrna/truseq-rna-sample-prep-v2-guide-15026495-f.pdf*. [Accessed 31 August 2017].

[36] Team RC. R: A language and environment for statistical computing. R Foundation for Statistical Computing. 2012; Available from: *URL http://www.R-project.org/*.

[37] Love MI, Huber W, Anders S. Moderated estimation of fold change and dispersion for RNA-seq data with DESeq2. *Genome Biol*, 2014; 15(12): 550.

[38] Mahmoud SM, Paish EC, Powe DG, Macmillan RD, Lee AH, Ellis IO, *et al.* An evaluation of the clinical significance of FOXP3+ infiltrating cells in human breast cancer. *Breast Cancer Res Treat*, 2011; 127(1): 99-108.

[39] Ft L, Ga R. Galectins as modulators of tumour progression. *Nat Rev Cancer*, 2005; 5(1): 29-41.

[40] Thomas DA, Massagué J. TGF-beta directly targets cytotoxic T cell functions during tumor evasion of immune surveillance. *Cancer Cell*, 2005; 8(5): 369-380.

[41] Gerlini G, Tun-Kyi A, Dudli C, Burg G, Pimpinelli N, Nestle FO. Metastatic melanoma secreted IL-10 down-regulates CD1 molecules on dendritic cells in metastatic tumor lesions. *Am J Pathol*, 2004; 165(6): 1853-1863.

[42] Kurte M, Lóez M, Aguirre A, Escobar A, Aguilló JC, Charo J, *et al.* A synthetic peptide homologous to functional domain of human IL-10 down-regulates expression of MHC class I and Transporter associated with Antigen Processing 1/2 in human melanoma cells. *J Immunol*, 2004; 173(3): 1731-1737.

[43] Nakanishi M, Rosenberg DW. Multifaceted roles of PGE in inflammation and cancer. *Semin Immunopathol*, 2013; 35(2): 123-137.

[44] Mellado M, De Ana AMN, Moreno MC, Martí Nez-A C, Rodrí Guez-Frade JM. A potential immune escape mechanism by melanoma cells through the activation of chemokine-induced T cell death. *Curr Biol*, 2001; 11(9): 691-696.

[45] Giovarelli M, Musiani P, Garotta G, Ebner R, Di Carlo E, Kim Y, *et al.* A "stealth effect" adenocarcinoma cells engineered to express TRAIL elude tumor-specific and allogeneic T cell reactions. *J Immunol*, 1999; 163(9): 4886-4893.

[46] Luo JL, Maeda S, Hsu LC, Yagita H, Karin M. Inhibition of NF-kappaB in cancer cells converts inflammation-induced tumor growth mediated by TNFalpha to TRAIL-mediated tumor regression. *Cancer Cell*, 2004; 6(3): 297-305.

[47] Evelkabler K, Song XT, Aldrich M, Huang XF, Chen SY. SOCS1 restricts dendritic cells' ability to break self tolerance and induce antitumor immunity by regulating IL-12 production and signaling. *J Clin Invest*, 2006; 116(1): 90.

[48] Mahmoud SM, Paish EC, Powe DG, Macmillan RD, Grainge MJ, Lee AH, *et al.* Tumor-infiltrating CD8+ lymphocytes predict clinical outcome in breast cancer. *J Clin Oncol*, 2011; 29(15): 1949.

[49] Jinno H, Hiraiwa K, Nakamura T, Saito J. Predictive and prognostic value of tumor-infiltrating lymphocytes in breast cancer treated with neoadjuvant chemotherapy. *J Clin Oncol*, 2015; 33(28_suppl): 128.

[50] Jiao S, Xia W, Yamaguchi H, Wei Y, Chen MK, Hsu JM, *et al.* PARP Inhibitor Upregulates PD-L1 Expression and Enhances Cancer-Associated Immunosuppression. *Clin Cancer Res*, 2017; 23(14): 3711.

[51] Nolan E, Savas P, Policheni AN, Darcy PK, Vaillant F, Mintoff CP, *et al.* Combined immune checkpoint blockade as a therapeutic strategy for BRCA1-mutated breast cancer. *Sci Transl Med*, 2017; 9(393).

[52] Curran MA, Montalvo W, Yagita H, Allison JP. PD-1 and CTLA-4 combination blockade expands infiltrating T cells and reduces regulatory T and myeloid cells within B16 melanoma tumors. *P Natl Acad Sci USA*, 2010; 107(9): 4275-4280.

[53] Nishikawa H, Sakaguchi S. Regulatory T cells in cancer immunotherapy. *[Rinshō ketsueki] Jpn J Clin hematol*, 2014; 55(10): 2183-2189.

[54] Khan S, Burt DJ, Ralph C, Thistlethwaite FC. Tremelimumab (anti-CTLA4) mediates immune responses mainly by direct activation of T effector cells rather than by affecting T regulatory cells. *Clin Immunol*, 2011; 138(1): 85-96.

[55] Kavanagh B, O'brien S, Lee D, Hou Y, Weinberg V, Rini B, *et al.* CTLA4 blockade expands FoxP3+ regulatory and activated effector CD4+ T cells in a dose-dependent fashion. *Blood*, 2008; 112(4): 1175.

[56] Wang H, Cheng F, Cuenca A, Horna P, Zheng Z, Bhalla K, *et al.* Imatinib mesylate (STI-571) enhances antigen-presenting cell function and overcomes tumor-induced CD4+ T-cell tolerance. *Blood*, 2005; 105(3): 1135-1143.

[57] Onizuka S, Tawara I, Shimizu J, Sakaguchi S, Fujita T, Nakayama E. Tumor rejection by in vivo administration of anti-CD25 (interleukin-2 receptor α) monoclonal antibody. *Cancer Res*, 1999; 59(13): 3128-3133.

[58] Huang B, Pan P-Y, Li Q, Sato AI, Levy DE, Bromberg J, *et al.* Gr-1+ CD115+ immature myeloid suppressor cells mediate the development of tumor-induced T regulatory cells and T-cell anergy in tumor-bearing host. *Cancer Res*, 2006; 66(2): 1123-1131.

[59] Ghiringhelli F, Puig PE, Roux S, Parcellier A, Schmitt E, Solary E, *et al.* Tumor cells convert immature myeloid dendritic cells into TGF-β–secreting cells inducing CD4+CD25+ regulatory T cell proliferation. *J Exp Med*, 2005; 202(7): 919-929.

[60] Gorelik L, Flavell RA. Immune-mediated eradication of tumors through the blockade of transforming growth factor-beta signaling in T cells. *Nat Med*, 2001; 7(7): 1118-1122.

[61] Neuzillet C, Tijerasraballand A, Cohen R, Cros J, Faivre S, Raymond E, *et al.* Targeting the TGFβ pathway for cancer therapy. *Pharmacol Therapeut*, 2015; 147: 22-31.

[62] Goeman JJ, van de Geer SA, de Kort F, van Houwelingen HC. A global test for groups of genes: testing association with a clinical outcome. *Bioinforma Oxf Engl*, 2004; 20(1): 93–9.